FLEROV LABORATORY OF NUCLEAR REACTIONS

In 2004, the FLNR scientific programme on heavy-ion physics included experiments on the synthesis of heavy and exotic nuclei using ion beams of stable and radioactive isotopes and studies of nuclear reactions, acceleration technology, and heavy-ion interaction with matter. These lines of investigations were represented in 15 laboratory and all-institute projects:

- Synthesis of new nuclei and study of nuclear properties and heavy-ion reaction mechanisms (9 projects);
- Radiation effects and modification of materials, radioanalytical and radioisotopic investigations using the FLNR accelerators (5 projects);
- Development of the FLNR cyclotron complex for producing intense beams of accelerated ions of stable and radioactive isotopes (2 projects);
- Development of the U400 + U400M + MT25 cyclotron–microtron complex for the production of radioactive ion beams (the DRIBs project).

In 2004, the operation time of the FLNR U400 and U400M cyclotrons was nearly 8000 hours, which is in accordance with the plan. Due to this, new experiments in low- and medium-energy ranges were possible.

Synthesis of New Elements

By employing the Dubna Gas-Filled Recoil Separator, the dependence of the production cross sections of the isotopes $^{286-288}114$ on the excitation energy of the compound nucleus $^{290}114$ at four energies of ^{48}Ca projectiles was studied (see Fig. 1). The properties of $^{286-288}114$ and their α-decay descendants coincide in full with those determined previously in cross bombardment reactions $^{244}\mathrm{Pu}(^{48}\mathrm{Ca}, 4{-}5n)^{287,288}114$, $^{245}\mathrm{Cm}(^{48}\mathrm{Ca}, 2{-}3n)^{290,291}116 \xrightarrow{\alpha} {}^{286,287}114$ and $^{249}\mathrm{Cf}(^{48}\mathrm{Ca}, 3n)^{294}118 \xrightarrow{\alpha} {}^{290}116 \xrightarrow{\alpha} {}^{286}114$ [1].

The even–odd isotope $^{287}114$ undergoes mostly sequential α-α-SF decay with a typical total decay time of about 2–20 s. The SF nuclide $^{279}110$ undergoes α decay with a probability of about 10% which ends with spontaneous fission of ^{271}Sg and ^{267}Rf. Their long lifetimes are caused by the influence of the deformed shells at $Z = 108$ and at $N = 162$.

During December 2003 through February 2004, the excitation function of evaporation of three and four neutrons in the reaction $^{238}\mathrm{U} + {}^{48}\mathrm{Ca}$ [2] was measured at three energies of ^{48}Ca (Fig. 1).

The investigation of the reaction $^{233}\mathrm{U} + {}^{48}\mathrm{Ca}$ opened for the first time a possibility of applying the method of genetic correlations for the identification of products in the reaction between ^{48}Ca and the actinide target. Here the evaporation of two to four neutrons leads to the known nuclide $^{277}112$ and to $^{278,279}112$, whose α decays lead to the known ^{270}Hs and ^{263}Rf. However, the calculated fission barriers of the nuclei to be produced in this reaction are considerably lower than those of the heavier ones, which should result in a corresponding decrease in the production cross sections. Indeed, the reaction cross section appeared to be below 0.6 pb, which supports the hypothesis concerning the influence of stability (or fission barriers) of nuclei on their production cross sections.

In April–May 2004 the irradiation of $^{248}\mathrm{Cm}$ with ^{48}Ca ions was performed. In 2000–2001 the first three atoms of element 116, $^{293}116$, were synthesized in this reaction. In the latest experiment the higher energy of ^{48}Ca was used which resulted in a considerable increase in the reaction cross sections (Fig. 1). Six decays of the new even–even isotope $^{292}116$ ($E_\alpha = 10.66$ MeV, $T_\alpha = 18$ ms) were observed.

The observed decay properties of the four isotopes of element 114 with masses 286–289 provide a consistent mass identification for all the heavier even-Z nuclei, in particular, the four isotopes of element 116 with masses 290–293 that were synthesized earlier in the reactions $^{245,248}\mathrm{Cm} + {}^{48}\mathrm{Ca}$, and also the isotope of element 118 with $A = 294$ observed as an α-α-SF chain in the reaction $^{249}\mathrm{Cf} + {}^{48}\mathrm{Ca}$. They also determine the masses of neutron-rich nuclei with $Z = 104{-}108$ which appear in the decay chains of the mother nucleus $^{287}114$. On the whole, they give a consistent pattern of decay of

the 18 even-Z neutron-rich nuclides with $Z = 104-118$ and $N = 163-177$.

The decay properties of nuclei in the decay chain $^{290}116 \xrightarrow{\alpha} {}^{286}114(\alpha/\mathrm{SF}) \xrightarrow{\alpha} {}^{282}112(\mathrm{SF})$, synthesized individually in the three reactions ^{245}Cm, ^{242}Pu, $^{238}\mathrm{U} + {}^{48}$Ca, coincide closely with those measured for the descendant nuclei of the heavy even–even nuclide $^{294}118$ produced in the reaction $^{249}\mathrm{Cf}(^{48}\mathrm{Ca}, 3n)^{294}118$.

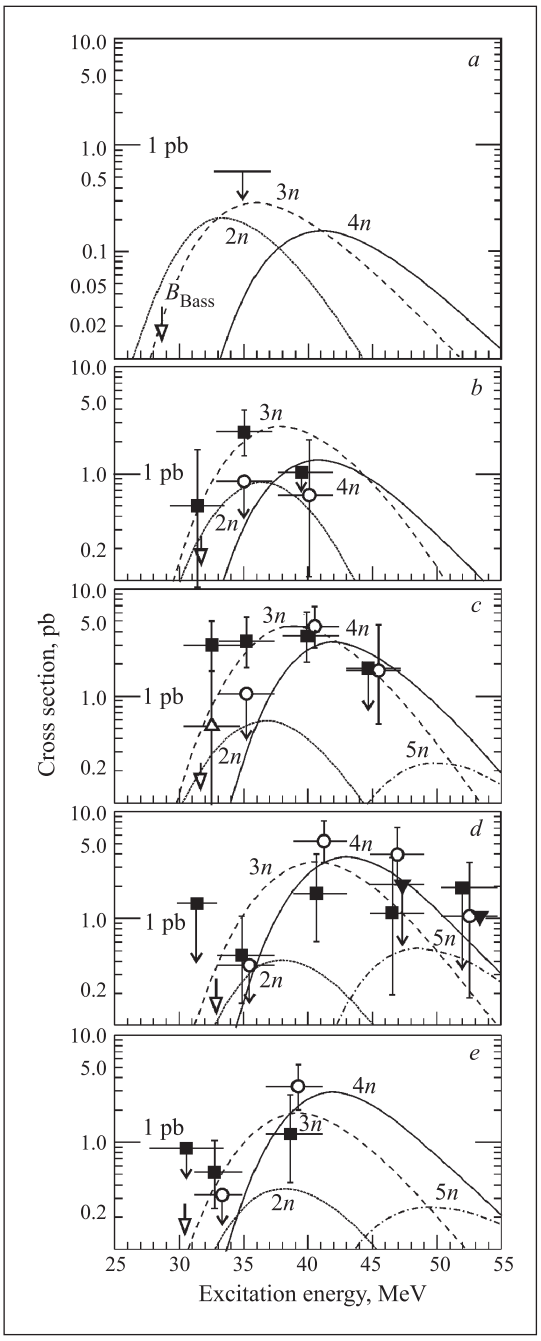

Fig. 1. Excitation functions for the $2n$ (△), $3n$ (■), $4n$ (○) and $5n$ (▼) evaporation channels from the complete-fusion reactions $^{48}\mathrm{Ca} + {}^{233}\mathrm{U}$ (*a*), ^{238}U (*b*), ^{242}Pu (*c*), ^{244}Pu (*d*), and ^{248}Cm (*e*)

All the observed α-decay sequences end in SF characterized by a high TKE of the fragments. For superheavy nuclei with $Z \geqslant 110$, the value of TKE increases with Z following the dependence of TKE vs. $Z^2/A^{1/3}$ expected for asymmetric fission. Spontaneous fission of the nuclei with $Z = 106$ and $N = 165$, as well as $^{267,268}\mathrm{Db}$ ($N = 162, 163$) with an abnormally high kinetic energy release, is most probably associated with the symmetric fission decay mode.

The production cross sections in the complete fusion reactions with ^{48}Ca are determined by the survivability of the nuclei and depend mostly on their fission barrier height. The expected increase in the fission barrier heights on approaching the neutron shell at $N = 184$ leads to an increase in the evaporation residue cross section; the conclusion is supported by experimental data (see Fig. 2). Thus, the effect of nuclear shells in the domain of superheavy elements results not only in substantially higher stability to various decay modes, but also in an increase in the production cross section for complete fusion reactions with ^{48}Ca projectiles. The observed 3–5 MeV upward shift of the maxima of the evaporation residue yields in the reactions of actinide nuclei with ^{48}Ca projectiles with respect to the calculated Coulomb barrier for spherical nuclei can be attributed to the selection of the entrance states associated with the orientation of the deformed target nuclei in collisions with ^{48}Ca.

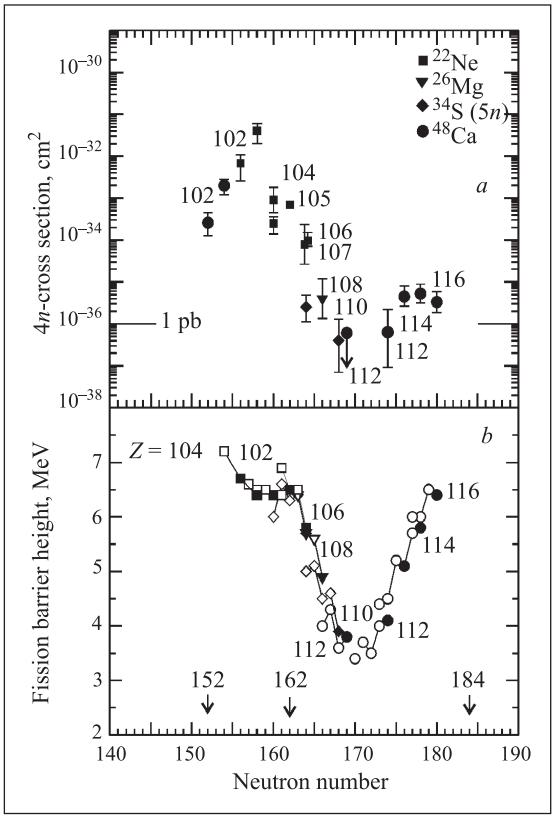

Fig. 2. Comparison of hot fusion cross sections for the production of $Z \geqslant 102$ nuclides (*a*) and the fission barrier heights as a function of neutron number (*b*). Solid symbols correspond to the number of neutrons in compound nuclei formed in different reactions

The present experimental data on the production cross sections and decay properties of even-Z nuclides can be used for determining conditions for the synthesis and prediction of the decay properties of odd-Z nuclides. Our interpretation of the data from the experiments on the synthesis of element 115 in the reactions $^{243}\mathrm{Am}(^{48}\mathrm{Ca}, 3{-}4n)^{288,287}115$ [3] is in agreement with the results of the recent experiments.

Chemistry of Transactinides

The recent discovery of elements 115 and 113 in the reaction $^{48}\mathrm{Ca} + {}^{243}\mathrm{Am}$ [3] was confirmed by an independent radiochemical experiment based on the identification of the long-lived decay product dubnium [4].

All of the new nuclides were synthesized in ^{48}Ca-induced reactions employing physical techniques. Their identification is based on their radioactive decay properties and the reaction mechanism, in particular, on the characteristic dependence of the yield of neutron-evaporation products on the excitation energy of the compound nucleus. The chemical identification of isotopes could give the identity of the atomic numbers of nuclei and provide independent evidence for the discovery of a new element.

An isotope of element 115 with mass number 288 was synthesized in the reaction $^{48}\mathrm{Ca} + {}^{243}\mathrm{Am} \rightarrow {}^{288}115 + 3n$. It undergoes five sequential α decays ($115 \xrightarrow{\alpha} 113 \xrightarrow{\alpha} 111 \xrightarrow{\alpha} 109 \xrightarrow{\alpha} 107 \xrightarrow{\alpha} 105 \xrightarrow{\mathrm{SF}}$) ending with the spontaneous fission of ^{268}Db. The half-life of the spontaneously fissioning final nucleus ^{268}Db was estimated from the three observed events to be $T_{1/2} = 16^{+19}_{-6}$ h. For chemical identification, the element should be separated according to its group properties.

According to the atomic configuration in the ground state ([Rn]$5d^{14}6p^37s^2$), Db should belong to the 5th group of the Periodic Table as a heavier homologue of Nb and Ta. Bearing in mind that the $Z = 105$ isotope of interest undergoes SF, we paid special attention to separating the group-5 elements from the actinides and, most importantly, from spontaneously fissioning isotopes of californium, ^{252}Cf ($T_{1/2} = 2.65$ y, SF — 3.1%) and ^{254}Cf ($T_{1/2} = 60.5$ d, SF — 99.7%). The separation from the actinides including Lr simultaneously answers the question if ^{268}Db undergoes an additional decay followed by spontaneous fission of ^{264}Lr.

The experiment was performed at the FLNR (JINR) U400 cyclotron in June 2004. The principal scheme of the set-up for target irradiation is shown in Fig. 3.

The 32-cm^2 rotating target consisted of the enriched isotope ^{243}Am (99.9%) in the oxide form deposited onto 1.5-μm Ti foils to a thickness of 1.2 mg/cm^2 of ^{243}Am. The target was bombarded by ^{48}Ca ions with an energy corresponding to 247 MeV in the middle of the target with an average intensity of $5{\cdot}10^{12}$ ion/s. The recoiling reaction products on leaving the target passed through a 12-mm collimator positioned 10 mm from the target, and were stopped in the 50-mm-diameter copper catcher block. A total of eight similar experimental runs with duration between 20 to 45 h were performed.

For each run, after the end of irradiation, a 7- to 10-μm layer (120–180 mg of Cu) was cut from the surface using a microlathe. The copper chips were dissolved in concentrated HNO_3. For the spectrometric control of the procedure of isolation of the group-5 elements and actinides, aliquots of nitrate solutions containing ^{92m}Nb, ^{177}Ta, ^{169}Yb and ^{167}Tm were added to the solution. From spectrometric measurements with irradiated sources, ^{92m}Nb and ^{177}Ta were isolated with efficiencies of $(85 \pm 5)\%$ and $(75 \pm 5)\%$, respectively, with suppression of the actinides by a factor of $\geqslant 8{\cdot}10^3$.

The chemical procedure took 2 to 3 h, starting from the end of irradiation until the beginning of detector measurements. For the registration of α particles and spontaneous fission fragments, the sample under study was placed between two semiconductor detectors which were positioned inside a neutron detector registering spontaneous fission neutrons. The efficiency of detecting fission fragments in the semiconductor detectors was about 90% and neutrons were detected with an average efficiency of about 40%. In the course of the 330-h test run performed before the experiment, no background SF events were detected.

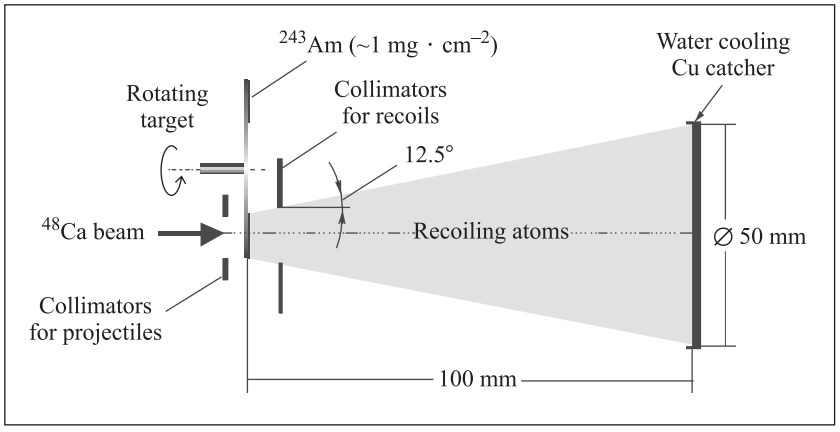

Fig. 3. The scheme of a set-up for the ^{243}Am target irradiation and collection of recoiling products

During eight runs of irradiating the ^{243}Am target with ^{48}Ca ions (with a total beam dose of $3.4 \cdot 10^{18}$), we detected 15 spontaneous fission events. The measurements were carried out for a total of 957 h.

The half-life of 32^{+11}_{-7} h determined from the time distribution of SF events agrees with the half-life obtained in the physical experiment within statistical errors. The total kinetic energy of the fission fragments ($\overline{\text{TKE}}$) was about 235 MeV. This result also agrees with the data from the physical experiment ($\overline{\text{TKE}} \sim 225$ MeV). The average neutron multiplicity per fission was $\nu \sim 4.2$. Both parameters, i.e., the high $\overline{\text{TKE}}$ value and the high neutron multiplicity, give evidence for the fission of a rather heavy nuclide. For comparison, in the spontaneous fission of ^{248}Cm, $\overline{\text{TKE}} = 181$ MeV and $\nu = 3.14$ and in ^{252}Cf, $\overline{\text{TKE}} = 185$ MeV and $\nu = 3.75$.

From the yield of spontaneously fissioning nuclei, one can determine the cross section of the parent nucleus — element 115 — as an evaporation product from the reaction $^{243}\text{Am} + {}^{48}\text{Ca}$. According to our data this formation cross section is about 4 pb. This agrees with the value ($\sigma_{3n} \sim 3$ pb) measured in the experiments with the gas-filled separator.

Thus, the data from the present experiment are the independent evidence for the synthesis of element 115, as well as element 113, in the reaction $^{243}\text{Am} + {}^{48}\text{Ca}$.

MASHA Separator

The manufactured separator was installed in a special testing room at FLNR. Tests of the whole set-up are underway now with a plasma ion source FEBIAD and a specially designed ECR ion source. In experiments with the plasma ion source the mass resolution $M/\Delta M$ of $3{\cdot}10^{-4}$ was achieved for Xe and Hg isotopes (Fig. 4).

The MASHA set-up surpasses all known facilities in efficiency of the superheavy atom production and in extracting information on their masses and decay characteristics. It also opens up new possibilities for the study of chemical properties of superheavy elements.

It should be noted that, due to the high efficiency of the chemical separation of the reaction products and the possibility of employing relatively thick target layers, the yield of the isotopes of superheavy elements is about a factor of five higher than that obtained with kinematic separators. This will allow us to use the MASHA set-up off-line for precise mass determination of the $^{48}\text{Ca} + {}^{243}\text{Am}$ reaction products. First experiments with the use of this separator and a ^{48}Ca beam of the U400 cyclotron are scheduled for 2005.

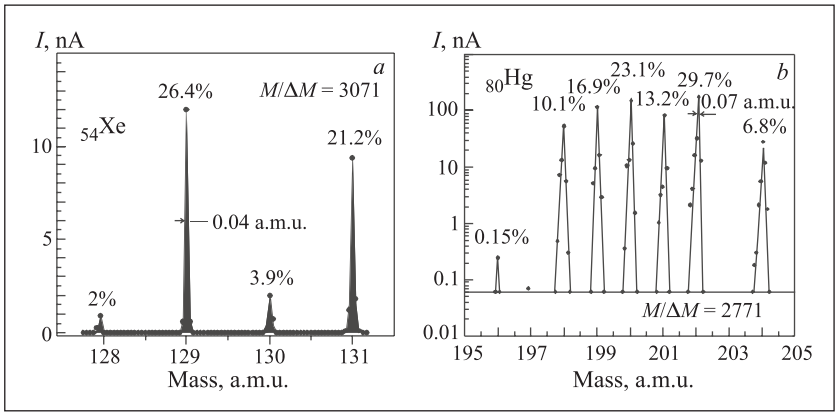

Fig. 4. Mass spectra of natural Xe (*a*) and Hg (*b*) isotopes produced with the MASHA separator

Nuclear Fission

The main task in 2004 was to carry out experiments aimed at understanding the dynamics of the process of formation and decay of superheavy nuclei with $Z = 116{-}122$. The main attention was paid to the influence of the entrance channel, evolution of the compound nucleus shape, from the moment of its formation to the scission point, and the competition between different exit channels (fission, quasi-fission, formation of the evaporation residue). Measurements of the angular, mass and energy distributions of fission fragments allowed us to obtain information on the process of the compound nucleus fusion–fission, as well as on the process of quasi-fission. The cross sections of these two processes were determined.

In 2004, the experimental data obtained in the study of mass–energy distributions of fission fragments and the excitation functions of superheavy nuclei with $Z = 102{-}122$, formed in the reactions $^{26}\text{Mg} + {}^{248}\text{Cm}$; $^{48}\text{Ca} + {}^{208}\text{Pb}$, ^{232}Th, ^{238}U, ^{244}Pu, ^{248}Cm; $^{58}\text{Fe} + {}^{208}\text{Pb}$, ^{232}Th, ^{244}Pu, ^{248}Cm at energies close to or below the Coulomb barrier, were analyzed. A series of experiments were carried out at FLNR with the use of the double-arm time-of-flight spectrometer CORSET. As a result of the experiments, a strong manifestation of shell effects in the quasi-fission fragments of nuclei with $Z = 112{-}122$ due to the influence of the shells with $Z = 28$ and $N = 50$ in the light fragment and those with $Z = 28$ and $N = 126$ in the heavy fragment was discovered.

As a result of the analysis of mass distributions (MD) of fragments of the superheavy nucleus ($Z = 102-122$) fission, a decomposition of the fusion–fission and quasi-fission contributions was performed. It was found that the mass distribution of fission fragments of compound nuclei with $Z = 112-122$ is asymmetric, with the light fission fragment mass $M_L \approx 132-134$ a.m.u. Thus, in the fission of superheavy nuclei the asymmetry of mass distribution is determined by the spherical shell of the light fragment, i.e., by the doubly magic tin ($Z = 50$, $N = 82$), in contrast to the fission of actinide nuclei, in which the MD asymmetry is determined by the deformed shell of the heavy fragment with $M_H \approx 140$ a.m.u. [5].

The competition between processes of fusion–fission and quasi-fission of supeheavy nuclei was studied in dependence on the entrance reaction channel and the shell structures of colliding nuclei and formed compound nucleus. For the reactions with ^{48}Ca ions a systematization of relations between fusion and quasi-fission cross sections as a function of mass of the formed composite nucleus was made. It was found that the contribution of quasi-fission decreases greatly in the case of the reactions in which magic spherical nuclei were used as targets. For the superheavy nuclei ^{274}Hs and ^{256}No a phenomenon of the multimodal fission was discovered at low excitation energies.

In the framework of the collaboration with LNL (Legnaro, Italy), investigations of fission and evaporation residue formation cross sections were continued. Also, mass–energy and angular distributions of fission fragments of ^{192,202}Pb produced in the reactions $^{48}\mathrm{Ca} + {}^{144,154}\mathrm{Sm}$ were measured (Fig. 5) [6]. In the reaction with a strongly deformed target ^{154}Sm, an asymmetric component was discovered in the mass distribution of fission fragments at energies close to or below the Coulomb barrier. The yield of this component increases with a decrease in the excitation energy. The angular distribution for this component is strongly asymmetric, which confirms the quasi-fission nature of the component. In the case of the spherical target ^{154}Sm the latter was not found.

Mass-angular distributions of fission and quasi-fission fragments were experimentally measured in the reactions $^{44}\mathrm{Ca}+{}^{206}\mathrm{Pb} \to {}^{250}\mathrm{No}$, $^{64}\mathrm{Ni}+{}^{186}\mathrm{W} \to {}^{250}\mathrm{No}$ at energies close to the Coulomb barrier. A strong manifestation of the quasi-fission component was observed in the more symmetric reaction $^{64}\mathrm{Ni} + {}^{186}\mathrm{W} \to {}^{250}\mathrm{No}$ as compared with $^{44}\mathrm{Ca} + {}^{206}\mathrm{Pb} \to {}^{250}\mathrm{No}$ (Fig. 6). From the analysis of the mass–energy distributions it

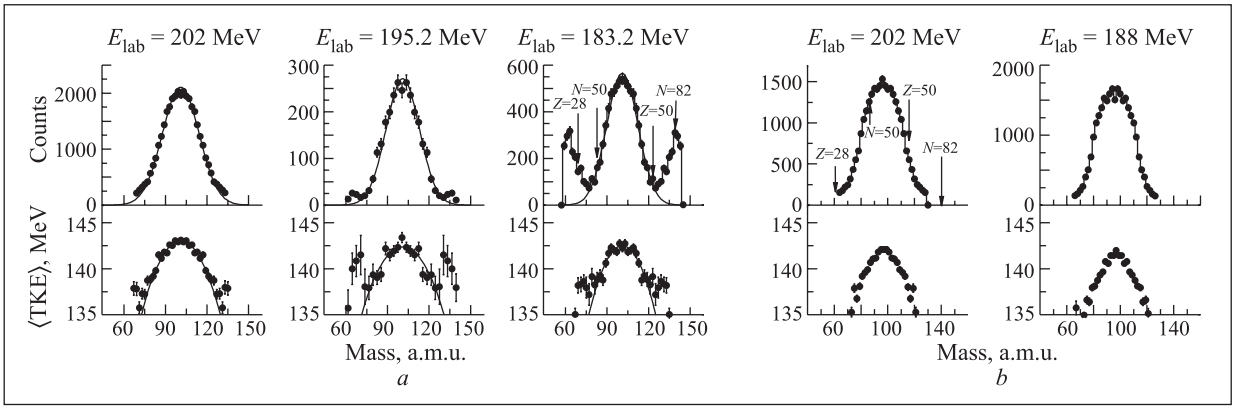

Fig. 5. Fission fragment mass–energy distributions at different ^{48}Ca energies for the $^{48}\mathrm{Ca} + {}^{154}\mathrm{Sm} \to {}^{202}\mathrm{Pb}$ (*a*) and $^{48}\mathrm{Ca}+{}^{144}\mathrm{Sm} \to {}^{192}\mathrm{Pb}$ (*b*) reactions

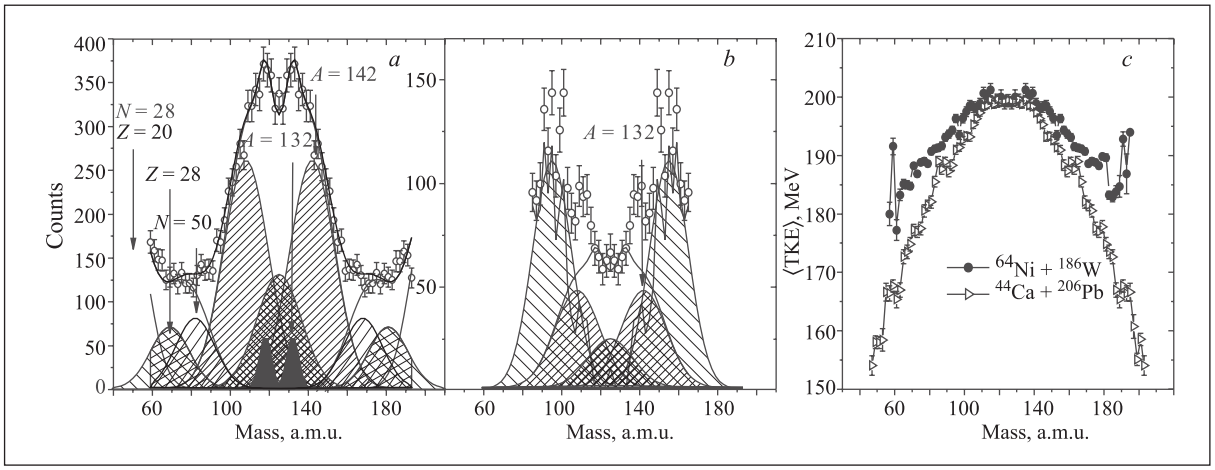

Fig. 6. Mass distributions for the $^{44}\mathrm{Ca} + {}^{206}\mathrm{Pb}$ (*a*) and $^{64}\mathrm{Ni} + {}^{186}\mathrm{W}$ (*b*) reactions and average kinetic energies ⟨TKE⟩ as a function of fragment mass (*c*) for these reactions at an excitation energy of 30 MeV

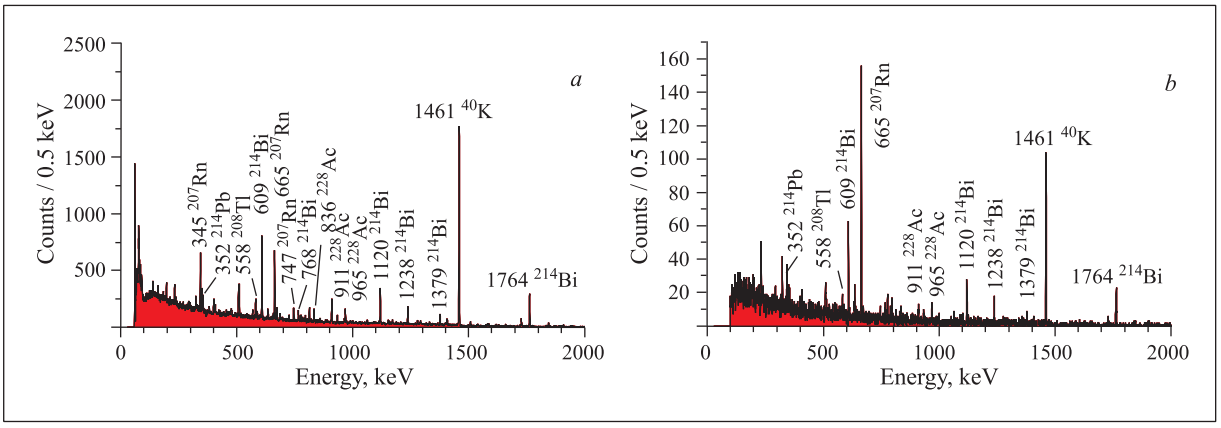

Fig. 7. *a*) An example of the recorded γ spectra by one Ge detector with BGO anti-Compton cleaning; *b*) the same spectrum using the ER–γ correlation analysis for the reaction $^{48}\mathrm{Ca} + {}^{164}\mathrm{Dy} \to {}^{212}\mathrm{Rn}^*$

follows that only a small part of the fragment yield ($\sim 25\%$) may be associated with the fusion–fission of the compound nucleus in the reaction $^{64}\mathrm{Ni} + {}^{186}\mathrm{W}$, the quasi-fission process being the major decay channel, whereas for the reaction $^{44}\mathrm{Ca} + {}^{206}\mathrm{Pb}$ about 70% of the total number of events can be attributed to the fission of the $^{250}\mathrm{No}$ compound nucleus.

VASSILISSA Separator

A new detector system was designed to measure decay properties of reaction products transported to the focal plane of the recoil separator VASSILISSA. It comprises a system of timing detectors composed of microchannel plates, as well as silicon and germanium detectors optimized for detecting the arrival of the reaction products and correlating with any subsequent radioactive decays, involving emission of α, β particles, γ rays, X rays and fission fragments.

The aim of the project is to benefit from the unique radioactive actinide targets available at Dubna and from the very intense stable beams provided by the U400 cyclotron. It will be thus possible for the first time to study nuclei above $Z = 100$ along an isotopic chain approaching $N = 162$.

The recoil nuclei were implanted into a stop 16-strip detector. In the backward direction, four electron detectors were placed. The focal plane detector was surrounded with seven Ge detectors.

To test the new detector together with electronic and data acquisition systems, the complete fusion reactions $^{48}\mathrm{Ca}{+}{}^{164}\mathrm{Dy} \to {}^{212}\mathrm{Rn}^*$, $^{40}\mathrm{Ar}{+}{}^{174}\mathrm{Yb} \to {}^{214}\mathrm{Ra}^*$ and $^{40}\mathrm{Ar}{+}{}^{181}\mathrm{Ta} \to {}^{221}\mathrm{Pa}^*$ were studied at the compound nucleus excitation energies corresponding to the de-excitation channels with the evaporation of 4–5 neutrons.

At a beam intensity of about 0.7 pμA the counting rate of scattered ions and other unwanted products at the focal plane detector was less than 50 Hz. The counting rate of background gammas at that beam intensity in a single Ge detector was about 1 kHz. With the use of anticoincidence with BGO anti-Compton shields the rate was reduced to 300 Hz. Figure 7 illustrates the γ spectra recorded for the reaction $^{48}\mathrm{Ca} + {}^{164}\mathrm{Dy} \to {}^{212}\mathrm{Rn}^*$. It is clearly seen how the ER–γ correlation analysis «cleans» the spectrum, and γ transitions from the isomeric state of $^{207}\mathrm{Rn}$ are well pronounced.

In the first full-scale experiment the complete fusion reactions $^{48}\mathrm{Ca} + {}^{207,208}\mathrm{Pb} \to {}^{255,256}\mathrm{No}^*$ and $^{48}\mathrm{Ca}{+}$ $^{209}\mathrm{Bi} \to {}^{257}\mathrm{Lr}^*$ were investigated. The decays of the isotopes $^{253,254,255}\mathrm{No}$ and $^{255}\mathrm{Lr}$ and their daughter products were studied. The data are now being analyzed.

Fragment Separator COMBAS

In 2004, a number of experiments were carried out at the in-flight separator COMBAS. They were devoted to the production of $^{13}\mathrm{B}$, $^{14}\mathrm{B}$, $^{15}\mathrm{B}$ radioactive beams and the study of the $^{11}\mathrm{B}$ cluster structure.

In the fragmentation reaction $^{18}\mathrm{O}$ ($35\,A\cdot\mathrm{MeV}$) + $^{9}\mathrm{Be}$, the production rates of neutron-rich nuclei $^{13}\mathrm{B}$ ($2 \cdot 10^6$ s^{-1}), $^{14}\mathrm{B}$ ($5 \cdot 10^5$ s^{-1}), $^{15}\mathrm{B}$ ($3 \cdot 10^5$ s^{-1}) were determined. They can be used in the studies of the cluster structure of these nuclei. The multidetector system consisting of 32-strip Si detectors was commissioned and installed in the COMBAS focal plane to register the coincidences of $^{11-15}\mathrm{B}$ breakup products. A multichannel electronic system and an appropriate data acquisition system were designed and manufactured to satisfy the demands of multiparticle spectroscopy measurements. Using the inelastic reaction $^{11}\mathrm{B}$ ($33\ A\cdot\mathrm{MeV}$) + $^{12}\mathrm{C}$ (0.28 mg/cm^2) $\to$ ($^{7}\mathrm{Li} + {}^{4}\mathrm{He}$) + $^{12}\mathrm{C}^*$, a test $^{11}\mathrm{B}^*$ breakup experiment was performed. The accumulated experimental data are now being processed and analyzed. Using the Quantum Molecular Dynamics (QMD) model (CHIMERA code), the simulations of velocity, isotopic and element distributions of fragmentation products from the reactions $^{18}\mathrm{O}$ ($35\,A\cdot\mathrm{MeV}$) + $^{9}\mathrm{Be}$ ($^{181}\mathrm{Ta}$) were performed and compared with the experimental data [7].

Earlier the observation of the ^{5}H ground-state resonance produced in the $^6\mathrm{He} + {}^1\mathrm{H}$ and $^3\mathrm{H} + {}^3\mathrm{H}$ reactions was reported. The two reactions yielded similar values, 1.7–1.8 MeV, for energy of the ^{5}H ground-state resonance. However, a discrepancy remained in the resonance widths — an unexpectedly small width of the resonance maximum ($\Gamma_{\mathrm{obs}} \leqslant 0.5$ MeV) was surprising. It prompted a further study of this nucleus.

Experiments aimed at the ^{5}H nucleus production were carried out at a triton beam energy of 58 MeV using the $t + t$ reaction in different kinematical conditions. In the present study, protons ejected in the reaction $^3\mathrm{H}(t,p)^5\mathrm{H}$ were detected in the range $\theta_{\mathrm{lab}} = 173{-}155°$, in CM system corresponding to a very backward direction branch (see the detector array in Fig. 8).

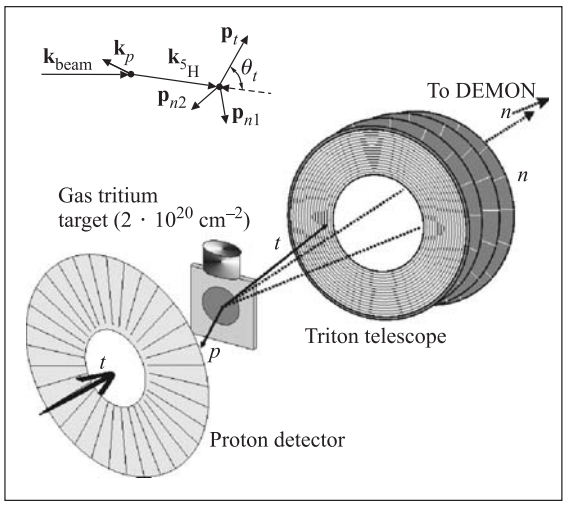

Fig. 8. The ACCULINNA detector array

Tritons and neutrons emitted in the ^{5}H decay were detected in coincidence with protons. Forty-nine DEMON modules installed in the forward direction detected at least one decay neutron with a high efficiency. The detection of the triple p–t–n coincidence unambiguously identified the outgoing reaction channel, making possible a complete kinematical reconstruction.

The $^5\mathrm{H}(t{+}2n)$ data in the centre-of-mass (CM) system are shown by diamonds in Figs. 9 and 10. The direction of the momentum transfer $\mathbf{k}_{\mathrm{beam}}{-}\mathbf{k}_p$ occurring in the reaction $^3\mathrm{H}(t,p)^5\mathrm{H}$ was chosen as the Z axis. The ^{5}H missing mass spectrum is shown in Fig. 9. Figure 10 shows the distribution of the ^{5}H decay energy between the relative motions in the $t{-}nn$ and nn subsystems (presented in terms of the $E_{nn}/E_{^5\mathrm{H}}$ ratio). It shows a narrow peak corresponding to a strong «dineutron» final-state interaction.

The most striking result is the observation of a sharp oscillating picture in the triton angular distribution. Such correlations can be obtained only for very specific conditions. The bulk of the data observed in these experiments can be explained only by the assumption that the direct transfer of two neutrons ($\Delta L = 2$, $\Delta S = 0$) dominates in the $^3\mathrm{H}(t,p)^5\mathrm{H}$ reaction, leading to the population of the broad overlapping $3/2^+$ and $5/2^+$ states in ^{5}H. According to theory prediction, one can consider these excited states as degenerative ones.

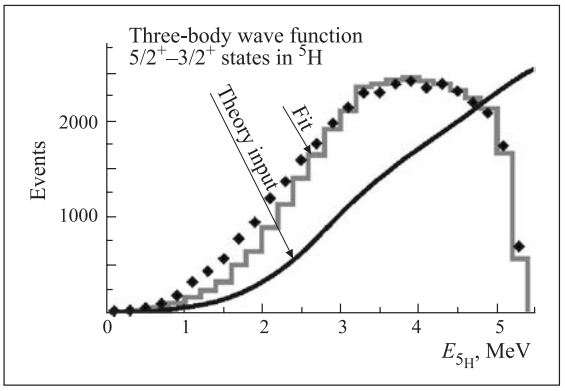

Fig. 9. A missing mass spectrum of ^{5}H

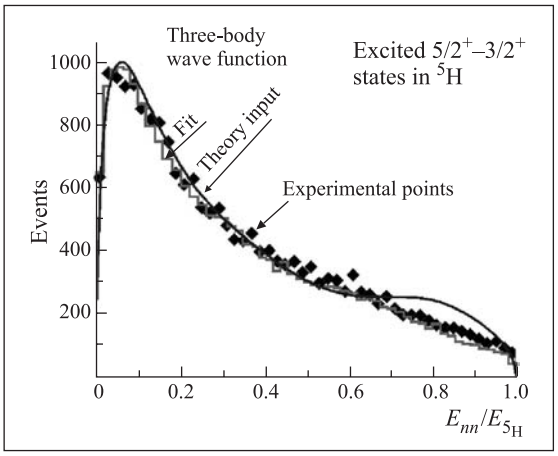

Fig. 10. A spectrum of relative energy for two neutrons

The following procedure was employed for data analysis. The correlations occurring at the ^{5}H decay are described as $W = \sum_{JM,J'M'} \langle J'M' |\rho| JM\rangle \times A^*_{J'M'} A_{JM}$. Here J, M are the total ^{5}H spin and its projection, A_{JM} are the decay amplitudes depending on the ^{5}H decay dynamics. $\langle J'M'|\rho|JM\rangle$ is the density matrix, which describes the polarization of the ^{5}H states populated in the reaction and takes into account the mixing of the $3/2^+$ and $5/2^+$ states. The amplitudes A_{JM} were expanded over a limited set of hyperspherical harmonics (assumed to be the same for the $3/2^+$ and $5/2^+$ states) [8].

Agreement obtained between the data and the MC results is excellent at $E_{^5\mathrm{H}} > 2.5$ MeV. Below this energy, one could not achieve the agreement assuming the interference of only $3/2^+$ and $5/2^+$ states; one can reproduce the correlations obtained at $E_{^5\mathrm{H}} < 2.5$ MeV by assuming the interference of the $1/2^+$ ground state with the $3/2^+{-}5/2^+$ doublet. This can be regarded as an evidence for the population of the ^{5}H ground state lying at about 2 MeV.

The missing mass spectrum of ^{5}H obtained in recent experiments shows a broad structure above 2.5 MeV.

The observed strong correlation pattern allows one to identify unambiguously this structure as a mixture of the $3/2^+$ and $5/2^+$ states. Such a correlation is a rare phenomenon for transfer reactions involving particles with a nonzero spin and means that either the $3/2^+$ and $5/2^+$ states are almost degenerative or the reaction mechanism causes a very specific interference of these states.

The observation of a $T = 3/2$ isobaric spin state in ^{5}He could provide useful information on the energy and width of the ^{5}H ground-state resonance. Such an analog state in ^{5}He remained yet unknown. In the present study the ^{2}H(^{6}He, ^{3}He)^{5}H and ^{2}H(^{6}He, t)^{5}He reactions were explored, studied at a ^{6}He beam energy of 132 MeV, to observe the ground state in ^{5}H and the lowest $T = 3/2$ state in ^{5}He, both having the $(1s)^3(1p)^3$ configuration. These reactions correspond to the pickups of either a proton or a neutron from the α core of ^{6}He. The kinematics of these reactions is similar, and their relative yields are governed by the isospin selection rule.

Two telescopes were employed in the experiment aimed at this study. The first telescope detected reaction ejectives (^{3}He, t) emitted at lab angles of $(25 \pm 7)^\circ$, whereas the second telescope was used for decay particles emitted at $(16 \pm 11)^\circ$. These were the tritons that appeared after the decay of ^{5}H and ^{3}He nuclei, tritons or deuterons which could originate from different ^{5}He decay modes.

In the case of the ^{2}H(^{6}He, ^{3}He) reaction the data show a resonance at $E_{\rm obs} = (2.2 \pm 0.4)$ MeV with the width $\Gamma_{\rm obs} = 2.5$ MeV. It is conceivable to attribute the 2.2-MeV resonance to the ground state of ^{5}H.

The data obtained for the ^{2}H(^{6}He, t) reaction indicate that a resonance state in ^{5}He with the isobaric spin $T = 3/2$ located at the excitation energy $E_{\rm obs} = (22.1 \pm 0.3)$ MeV and having the width $\Gamma_{\rm obs} = (2.5 \pm 0.3)$ MeV was observed. It was found that that state appeared in the ^{5}He three-body decay modes allowed for the $T = 3/2$ state. The cross sections were estimated to be (0.10 ± 0.03) and (0.2 ± 0.1) mb/sr for the $^5\mathrm{He} \to {}^3\mathrm{He} + n + n$ and $^5\mathrm{He} \to t + p + n$ decay modes of the ^{5}He isobaric analog state, respectively.

Exotic Decay Modes. 4π Detector FOBOS

The major efforts of the FOBOS group during 2004 were concentrated on the study of a new type of nuclear transformation, namely collinear cluster tripartition (CCT) discovered earlier in our experiments at the FOBOS set-up. The new experimental facility, the Modified Mini-FOBOS set-up (MMF), was successfully put into operation. It was specially optimized for the investigation of the characteristics of the CCT decay channel of heavy nuclei, powered by the Transformable Neutron Skin (TNS) and equipped with the new electronic system for the identification of events in which two fragments hit one and the same detector in a short time interval. Two experiments were performed successfully at the MMF set-up in 2004 [9]. The analysis of the experimental data is in progress. Furthermore, the data measured with the FOBOS spectrometer some years ago were reanalyzed employing the new mathematical formalism specially developed. Clear confirmation of the CCT was obtained for the decays of ^{252}Cf (Fig. 11) and ^{248}Cm nuclei.

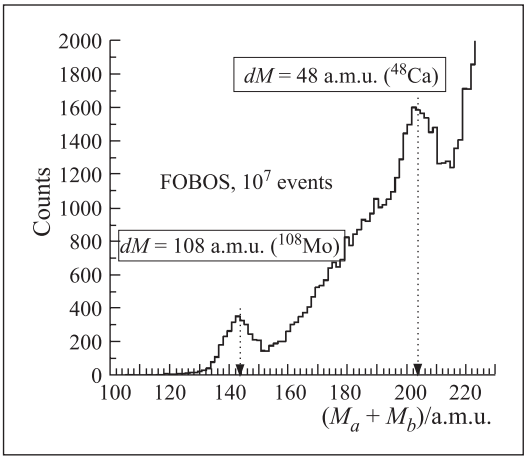

Fig. 11. A spectrum of the total mass of detected fission fragments of ^{252}Cf (sf)

Reactions Induced by Stable and Radioactive Ion Beams of Light Elements

At the U400M cyclotron, experiments were performed to measure the excitation functions of fusion reactions with a consequent evaporation of neutrons from the compound nucleus ^{215}At, produced in the reactions $^{208}\mathrm{Pb}(^7\mathrm{Li}, xn)^{215-xn}\mathrm{At}$ and $^{209}\mathrm{Bi}(^6\mathrm{He}, xn)^{215-xn}\mathrm{At}$ [10]. The excitation functions for the fission of the ^{215}At nucleus formed with both beams were also measured. The measurements were carried out in the projectile energy range of 7–25 MeV/nucleon. In the case of the ^{7}Li beam the excitation functions were obtained for the 3–9-neutron evaporation channels, whereas for the ^{6}He beam it were the 4- to 8-neutron evaporation channels (Fig. 12). The ^{6}He beam was produced as a secondary beam in the interaction of a ^{7}Li beam with a beryllium target. The experiments were performed using the multidetector set-up MULTI.

The comparative analysis of the excitation functions for the two studied reactions $^6\mathrm{He} + {}^{209}\mathrm{Bi}$ and $^7\mathrm{Li} + {}^{208}\mathrm{Pb}$ showed that those functions were identical within the experimental errors for a broad range of the excitation energy. This fact can serve as an evidence for the fact that in the interaction of the weakly bound nuclei ^{7}Li and ^{6}He at energies above the Coulomb barrier no peculiarities of the entrance channel are manifested and the decay of the formed compound nucleus is determined solely by its properties. The study of the excitation functions of these reactions at energies close to the Coulomb barrier will be continued at the DRIBs complex.

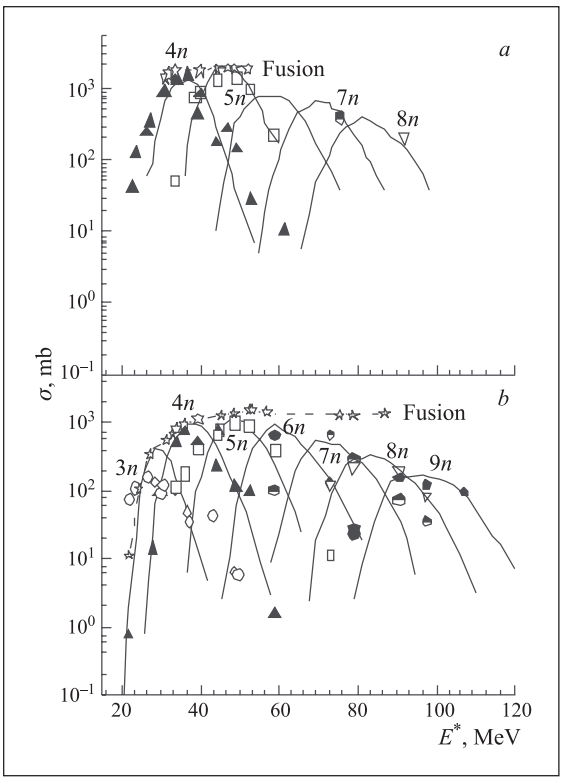

Fig. 12. Excitation functions for xn-evaporation channels and complete fusion in the $^{6}\mathrm{He} + {}^{209}\mathrm{Bi}$ (*a*) and $^{7}\mathrm{Li} + {}^{208}\mathrm{Pb}$ (*b*) reactions

Measurements were also carried out of the total reaction cross section σ_R for the $^{4,6}\mathrm{He} + {}^{28}\mathrm{Si}$ and $^{7}\mathrm{Li} + {}^{28}\mathrm{Si}$ reactions in the energy range 5–50 MeV/nucleon [11]. The experiments were made using the transmission method in a multilayer semiconductor telescope. The use of thin Si detectors 20–300 μm in thickness made it possible to measure the energy dependence σ_R with the energy resolution $\delta E \sim 1$ MeV/nucleon.

The analysis of the data revealed a peculiarity in the total reaction cross section for the $^{6}\mathrm{He} + {}^{28}\mathrm{Si}$ reaction in the energy range 10–20 MeV/nucleon; viz., the cross section exceeds the theoretical calculations by about 150–200 mb. This may be due to the manifestation of the single-particle interactions of neutrons, forming a halo, and the target protons.

Another series of experiments was dedicated to the investigation of the nuclear structure of fission fragments using the methods of resonance laser spectroscopy. A technique has been developed for measuring the quadrupole moments of the odd isotopes $^{93}\mathrm{Zr}$ and $^{95}\mathrm{Zr}$. These isotopes were produced by chemical separation from a uranium target, which had been irradiated by brehmsstrahlung at the FLNR microtron. The samples, obtained in this way, were studied in order to determine the quadrupole deformation of $^{93}\mathrm{Zr}$ and $^{95}\mathrm{Zr}$. The analysis of the experimental data is in progress and will allow determining the change of deformation with increasing neutron excess of the nuclei.

Theoretical and Computational Physics

A systematic analysis of reaction dynamics of the superheavy nucleus formation and decay at beam energies near the Coulomb barrier was performed [12]. Three-dimensional potential energy surfaces in the space of «elongation–deformation–mass asymmetry» were calculated and used for the analysis of SHE formation and quasi-fission processes within the model proposed earlier. The main attention was paid to the orientation effect in collisions of statically deformed nuclei and its influence on the heavy CN formation. It was shown that tip collisions lead the system mainly to the quasi-fission channels, whereas side collisions were more preferable for the formation of CN. This effect even more shifts the EvR excitation functions of SHE formation in the asymmetric fusion reactions induced by $^{48}\mathrm{Ca}$ to higher energies close to the Coulomb barriers of the side configurations.

Dynamical calculations were carried out using the Langevin equations combined with the statistical model for pre-scission neutron evaporation. Several projectile–target combinations leading to the formation of superheavy nuclei were studied within the model [13]. Mass distribution of fission and quasi-fission fragments was calculated and reasonable agreement with experimental data was obtained. Pre-scission neutron multiplicity was also calculated and compared with experimental data. Two components were found in the neutron distributions which may be attributed to the quasi-fission and regular fusion–fission processes. This fact could be very important for a further study of dynamical evolution of heavy nuclear systems.

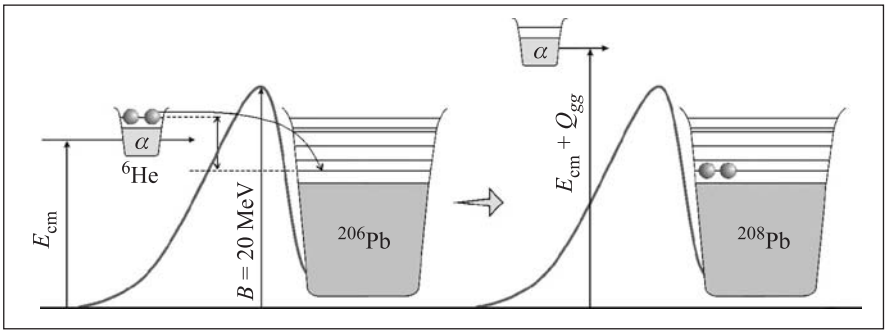

Fig. 13. A schematic view of sequential fusion of $^{6}\mathrm{He}$ with $^{208}\mathrm{Pb}$ at a subbarrier energy

A new mechanism, «sequential fusion», was proposed and studied for near-barrier fusion of weakly bound neutron-rich nuclei [14]. It was shown that intermediate neutron transfer with positive Q values might significantly enhance the fusion probability at subbarrier energies. In the process of «sequential fusion» intermediate neutrons are transferred to the states with $Q > 0$. In a certain sense, it is an «energy lift» for the two interacting nuclei (Fig. 13). The effect was found to be very profound, especially for the fusion of weakly bound nuclei. New experiments have been proposed, in which the effect will be clearly distinguished. In these experiments the near-barrier fusion reactions $^{6}\mathrm{He} + {}^{206}\mathrm{Pb}$ and $^{4}\mathrm{He} + {}^{208}\mathrm{Pb}$ leading to the same compound nucleus $^{212}\mathrm{Po}$ should be studied at the same subbarrier centre-of-mass energy (same temperature). At $E_{\mathrm{cm}} \sim 15$ MeV a probability of the formation of Po isotopes was predicted to be 100 times higher for $^{6}\mathrm{He} + {}^{206}\mathrm{Pb}$ as compared with $^{4}\mathrm{He} + {}^{208}\mathrm{Pb}$.

Heavy-Ion Interaction with Matter

The transmission electron microscopy (TEM) analysis of radiation defects with a «black-white» contrast discovered in silicon irradiated with high-energy (710 MeV) Bi ions was performed using the techniques of chemical and ionic removal of submicron layers. The chemical removal preserves the crystal structure of a pre-surface layer, while the ion dispersion, in contrast, forms an amorphous pre-surface layer. Thus, it was shown that along the ion track in silicon the high-energy bismuth ion causes formation of a cylindrical area with a destructive crystal lattice which is visualized in PEM as the so-called «black-white» contrast due to its deformation relaxation in the pre-surface crystal volume of silicon.

In the framework of the program for developing a technology of ion-track lithography, peculiar features of formation in a polymeric matrix (polycarbonate) of etched submicron structures with the high-aspect ratio (40:1) at the irradiation with high-energy (250 MeV) krypton ions through absorbing masks of a cylindrical form were realized and investigated.

Possibilities of forming a porous structure in polyimide films irradiated with ions were investigated. Structural and optical properties of track membranes on the basis of polypyromellitimide were investigated. The latter was suggested for using as radiation-proof filters of electromagnetic radiation in X-ray and ultraviolet ranges (in the structure of X-ray telescopes for research on a solar crown).

Research by making use of methods of atomic force microscopy on nanodimensional structural defects on a surface of Al_2O_3, MgO and $MgAl_2O_4$ monocrystals exposed to ions of krypton, xenon and bismuth with energies in the range of 0.6–3.5 MeV/nucleon were continued. The purpose of the work is to discover the laws of formation of structural defects on the surface of candidate materials of inert thinners (matrixes) of nuclear fuel caused by irradiation with heavy ions with energies characteristic of fission fragments. The upper limits were determined for the values of density of ionization in a pre-surface layer of the samples from which radiation-caused changes in the surface structure of the given crystals were registered. These threshold values are 25.4 keV/nm for sapphire, 15.8 keV/nm for magnesium oxide and 15.5 keV/nm for spinel.

Experiments were carried out on determining a level of mechanical stress in ruby monocrystals in the course of irradiation with 3–7 MeV/nucleon ions of argon, krypton and bismuth. The magnitude of the stress was determined on the R-lines shift in the spectra of luminescence generated by high-energy ions (piezospectroscopic effect) in the given material. It was found that the level of stress in the sample's layer irradiated with 710-MeV bismuth ions was not determined by the full concentration of defects formed in elastic collisions. A basic contribution to the formation of defective structures resulting in the appearance of compressing mechanical stress is made by electronic losses of the ion energy.

The influence of the irradiation with fast neutrons and ions of Kr (235 MeV) and Bi (710 MeV) on optical and electric properties 4H-SiC was investigated. In this work methods of photoluminescence and spectroscopy of deep levels were used. Electric characteristics of Al and Cr were studied using Shottky barriers. According to experimental data, neutrons and high-energy ions cause formation of identical defective centres in 4H-SiC. These results show that even at extremely high values of ionization density (34 keV/nm) the formation of a defect structure in silicon carbide monocrystals is determined by the losses of the particle energy for elastic scattering.

Employing the set-up «Migration» a number of physical and chemical characteristics of In^{+3}, Cd^{+2}, Zr^{+4}, Hf^{+4} and Pu^{+6} ions in water solutions were determined using isotopes ^{111}In, Cd, ^{88}Zr, ^{175}Hf and $^{237}\mathrm{Pu}$.

Physics and Heavy-Ion Accelerator Techniques

U400 Cyclotron. In 1998–2004, the U400 cyclotron was mainly used for the experiments with $_{48}\mathrm{Ca}^{5+}$ ions for the synthesis of superheavy elements. The essential modernization of the U400 axial injection included sharp shortening of the horizontal part of the injection channel. To increase the acceleration efficiency, a combination of line and sine bunchers was used. The modernization gave the possibility of increasing the $^{48}\mathrm{Ca}^{+5}$ current into the injection line from 40–60 to 80–100 μA. Correspondingly, the average output $^{48}\mathrm{Ca}^{+18}$ ion current was increased from 15 to 25 μA. A diagram of the U400 operation in 1997–2004 is shown in Fig. 14.

The modernization of U400 was proposed for the improvement of the cyclotron parameters. The cyclo-

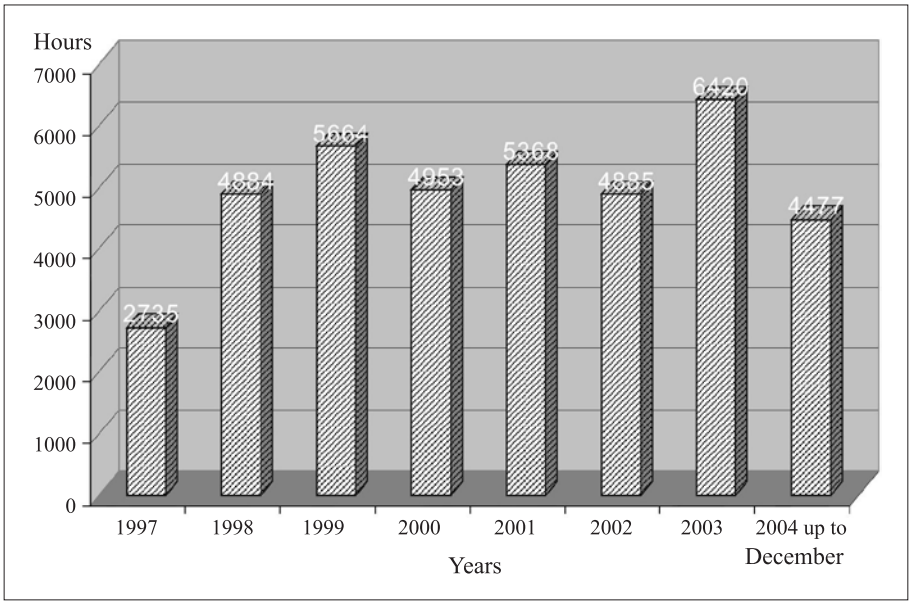

Fig. 14. A diagram of the U400 operation in 1997–2004

Parameters	U400	U400R
Electrical power of magnet power supply system, kW	850	200
The magnetic field level in the magnet centre, T	1.93–2.1	0.8–1.8
The A/Z range	5–12	4–12
The frequency range, MHz	5.42–12.2	5.42–12.2
The ultimate extraction radius, m	1.72	1.8
K factor	305–625	100–506
Vacuum level, Torr	$(1–5)\cdot 10^{-7}$	$(1–2)\cdot 10^{-7}$
Ion extraction method	Stripping foil	Stripping foil deflector
Number of directions for ion extraction	2	2

tron parameters before (U400) and after (U400R) the modernization are shown in table. The aims of the modernization were:

1. Decreasing the magnetic field level at the cyclotron centre from 1.93–2.1 to 0.8–1.8 T which allows us to decrease the electrical power of the U400R main coil power supply by a factor of 4.

2. Providing the fluent ion energy variation at the factor of 5 for every mass-to-charge ratio A/Z at an accuracy of $\Delta E/E = 5\cdot 10^{-3}$.

3. Increasing the intensity of accelerated ions of rare stable isotopes by a factor of 3.

The possibility of increasing the injection voltage from 13–20 to 40–50 kV is under study. As we estimated, the reconstruction can provide a 1.5–2 times increase in the U400R accelerating efficiency, it is particularly important for ^{48}Ca ions.

The RF system of U400R will consist of two RF generators that will excite two separated RF dee resonators. The RF resonators will be made from iron with copper coating to decrease the outgasing rate from the vacuum surface.

U400M Cyclotron. A diagram of the U400M operation in 1998–2004 is shown in Fig. 15.

Two sources of ions were installed at the U400M cyclotron: an ECR — for the production of heavy ions, and a high-frequency source of ions, which is used for the generation of tritium ion beam. The tritium ion beam was required for the study of ^{4}H and ^{5}H resonance states in the neutron transfer reactions $t + t \to {}^{5}\mathrm{H} + p$ and $t + t \to {}^{4}\mathrm{H} + d$. Experiments were performed at the ACCULINNA separator.

At the U400M cyclotron the tritium ions should be accelerated as molecular ions $(\mathrm{DT})^{+}$ from the point of view of beam extraction by stripping. The required beam intensity at the liquid tritium target was about 10^{8} pps. Taking into account the beam losses on transport and monochromatization, the intensity of the accelerated beam should be about 10 nA ($6\cdot 10^{10}$ pps).

The main requirements to the ion source were: minimal consumption of radioactive tritium; high output of molecular ions; long lifetime.

A RF ion source was chosen for the production of molecular ions (Fig. 16). During the operation at the test bench, the ion source was optimized for the production of H_2^{+} ions.

For feeding the tritium atoms into the ion source, a special gas feed system was developed at RFNC – VNIIEPh (Sarov, Russia) which provides fine regulation of the gas flow and safe handling with tritium.

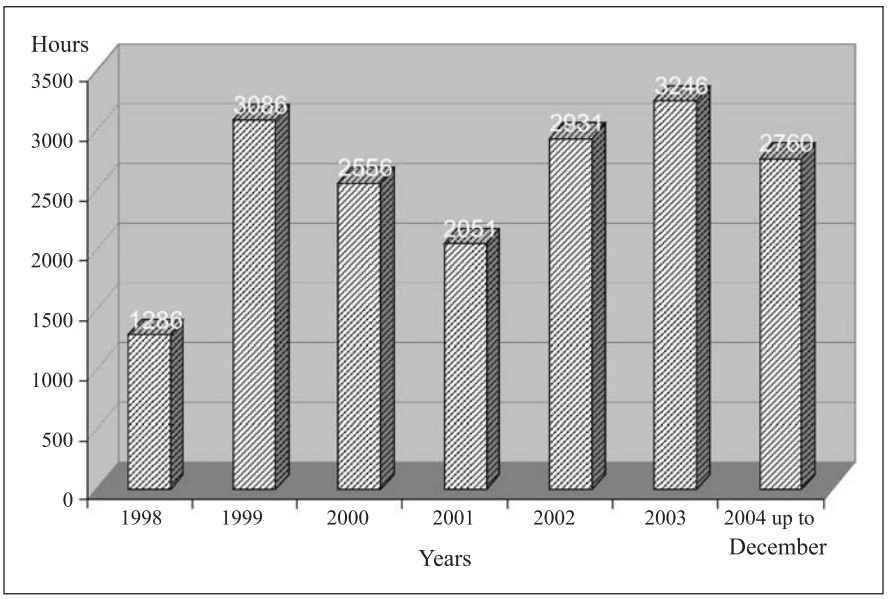

Fig. 15. A diagram of the U400M operation in 1998–2004

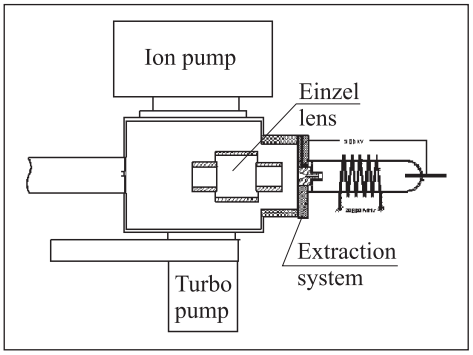

Fig. 16. A schematic view of the RF ion source

The hydrogen isotopes, including a deuterium–tritium mixture, are chemically kept on ^{238}U. After heating the uranium, the hydrogen isotopes flow into the buffer volumes. From the buffer volumes gases are fed into the ion source due to diffusion through the walls of a heated nickel capillary. Special attention was paid to the design of the vacuum system to provide its environmentally safe operation. A beam of 58-MeV tritons was produced at the U400M cyclotron and delivered to the tritium target of the ACCULINNA separator.

Accelerator Complex DRIBs. In 2003, the first stage of the DRIBs project was realized at the U400–U400M accelerator complex. The experiments with radioactive ^{6}He ions started in December 2004. The U400 cyclotron accelerated the secondary ^{6}He^{+} ions produced at U400M from an energy of 3.5 keV/a.m.u. to 5–20 MeV/a.m.u.

DC40 Cyclotron. The DC40 heavy-ion cyclotron has been in operation since 1985 to accelerate ions from C to Ar with a fixed energy of about 1.2 MeV/nucleon. For the generation of such ions the PIG ion source was used. Experiments in the field of solid-state physics and industrial applications require heavy ions up to Xe. In order to produce ions heavier than Ar with the given energy, we need a powerful ion source capable of generating highly charged intense heavy ions (e.g., Kr^{15+} and Xe^{23+}). To meet these demands, a superconducting (SC) ECR ion source (ECRIS) was built together with a new axial injection line.

The main feature of the ECRIS is using a small Gifford–McMahon refrigerator for cooling the solenoid coils down to 4.2 K. It maintains the superconductivity of the solenoid coils without using liquid He. The hexapole magnet consists of permanent magnets made of NdFeB with high residual magnetization ($B_r \sim 1.3$ T). The maximal induction of the mirror magnetic field is 2 and 3 T at the beam extraction and microwave injection side, respectively. The magnetic field induction at the inner surface of the plasma chamber is 1.2 T. The injected microwave frequency is 18 GHz, the maximal microwave power 1.5 kW. One of the first spectra of Kr ions, obtained with SC ECRIS, is given in Fig. 17.

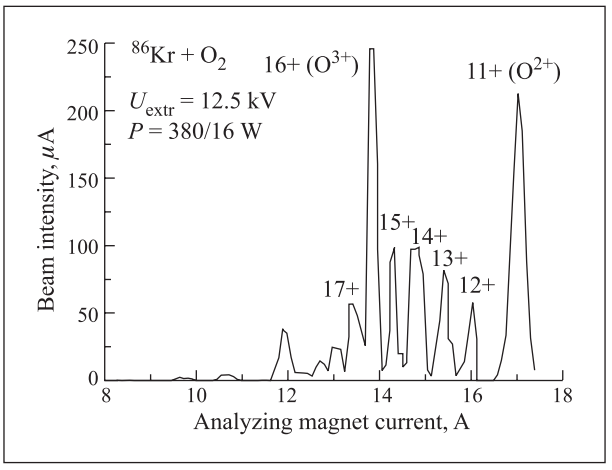

Fig. 17. A spectrum of Kr ions from SC ECRIS

At present, all principal cyclotron systems have been tested, and the tests gave good results. Recently the cyclotron has been commissioned and the first accelerated beam of Kr^{15+} has been extracted.

DC72 Cyclotron. Tests of the basic systems of the DC72 accelerator were carried out in accordance with the schedule for 2004. Magnetic measurements were carried out in full. The pumping-out of the channel of axial injection was done, tests of the water-cooling system were carried out, and projected parameters were achieved.

DC60 Cyclotron. A draft of the DC60 heavy-ion accelerator has been developed. The accelerator should provide intense beams of accelerated ions in the energy range from 0.35 to 1.67 MeV/nucleon, as well as ion beams from the ECR source with an energy of 25 keV/charge. This accelerator will be used for realization of the programme of fundamental and applied research. The main items are:

- track membranes and their applications,
- modification of the surface of materials,
- fundamental and applied aspects of formation and use of nuclear tracks in solids,
- ionic-implantation nanotechnology.

The project has passed the expertise at the Scientific Council of the Russian Academy of Sciences on charged particle accelerators.

REFERENCES

1. *Oganessian Yu. Ts. et al.* // Phys. Rev. C. 2004. V. 69. P. 054607.
2. *Oganessian Yu. Ts. et al.* // Ibid. V. 70. P. 064609.
3. *Oganessian Yu. Ts. et al.* // Ibid. V. 69. P. 021601(R).
4. *Dmitriev S. N. et al.* JINR Preprint E12-2004-157. Dubna, 2004.
5. *Itkis M. G. et al.* // Nucl. Phys. A. 2004. V. 734. P. 136.
6. *Trotta M. et al.* // Ibid. P. 245.
7. *Aleshin V. P. et al.* // Proc. of Intern. Symp. on Exotic Nuclei (EXON-2004), Peterhof, Russia, July 5–12, 2004 (in press).
8. *Grigorenko L. V. et al.* // Eur. Phys. J. A. 2004. V. 20. P. 419.
9. *Pyatkov Yu. V. et al.* JINR Preprint E15-2004-65. Dubna, 2004.
10. *Hassan A. A. et al.* JINR Preprint P15-2004-122. Dubna, 2004 (in Russian).
11. *Ugryumov V. Yu. et al.* // Nucl. Phys. A. 2004. V. 734. P. E53.
12. *Zagrebaev V. I.* // Nucl. Phys. A. 2004. V. 734. P. 164.
13. *Aritomo Y. et al.* // Prog. Theor. Phys. Suppl. 2004. V. 154. P. 449.
14. *Zagrebaev V. I.* // Ibid. P. 122.